Journal of Alloys and Compounds 509 (2011) 5183–5186

Contents lists available at ScienceDirect

Journal of Alloys and Compounds

journal homepage: www.elsevier.com/locate/jallcom

Power factor enhancement in Zn-doped $Na_{0.8}CoO_2$

P.H. Tsai [a], T.S. Zhang [a], R. Donelson [b], T.T. Tan [a], S. Li [a,*]

[a] School of Materials Science and Engineering, The University of New South Wales, Sydney, NSW 2052, Australia
[b] CSIRO Division of Process Science and Technology, Clayton, Victoria 3168, Australia

ARTICLE INFO

Article history:
Received 25 November 2010
Received in revised form 4 February 2011
Accepted 7 February 2011
Available online 15 February 2011

Keywords:
Na_xCoO_2
Zn-doped
Thermoelectric properties

ABSTRACT

The thermoelectric properties of $Na_{0.8}Zn_xCo_{1-x}O_2/(ZnO)_y$ ($x \leq 0.01$, $0 \leq y \leq 0.14$) have been systematically investigated. The results suggest that doping divalent Zn ions within solubility limit $x^* \sim 0.01$ leads to simultaneous reduction in resistivity and enhancement of thermopower. Analysis of the results show that the reduction of resistivity may be attributed to improved mobility of carriers, while the enhancement of thermopower may originate from the geometric relaxation of distorted CoO_6 octahedra caused by partial Zn substitution, leading to a narrower band width in the strongly correlated environment, consequently resulting in a remarkable 20% improvement in power factor.

1. Introduction

The upsurge of interest in *p*-type sodium cobaltates over the decade primarily stems from its superior thermoelectric (TE) properties and superconductivity [1,2]. Theoretical investigation on the origin of anomalously large thermopower using generalized Heikes formula has revealed the significance of the ratio, spin and orbital degrees of freedom of Co^{3+} and Co^{4+} ions [3]. This has been verified experimentally [4,5]. While the performance of sodium cobaltates is approaching its intrinsic limit, the introduction of "guest" atoms into the crystal (i.e. doping) provides alternative route for further enhancing the TE properties. Extensive investigation has been carried out on the partial substitution of various elements either into the Na or Co sites [6–19]. The latter includes tri- and tetravalent ions [16–19], as well as divalent ions such as Zn^{2+}, Ni^{2+} and Pd^{2+} [12–14]. However, since Ni and Pd may exist in several valence states, the transport mechanisms are difficult to analyze. The unique valence state of Zn^{2+}, on the other hand, provides excellent opportunity for investigating the influence of divalent substitution for Co on TE properties of the cobaltates. An earlier study on $Na_{0.8}Zn_xCo_{1-x}O_2$ found that a large thermopower S (~300 μV K^{-1} at 720 K) was achieved at the maximum solubility of $x^* \sim 0.05$ while a new phase, $Na_2Zn_2O_3$, appeared when $x > 0.05$ [13]. In contrast, a much higher x^* of ~0.15 was observed with a much lower S (~125 μV K^{-1} at 300 K) [14]. The high x^* reported from the latter group is interesting considering the relatively high standard enthalpy of formation of ZnO (i.e. −348 kJ mol^{-1}). However, the influence of Zn-substitution on the transport properties in $Na_{0.8}Zn_xCo_{1-x}O_2$ is still unclear. In present work, the mechanism of such an influence is investigated through a series of experiments in which Co^{3+} ions were partially substituted by Zn^{2+} in $Na_{0.8}CoO_2$ in a controlled fashion. The Zn-substitution effect on high-temperature TE properties was also studied systematically, thus revealing the subtle interplay between the electronic and crystallographic structures on the variations of TE properties that are associated with the Zn^{2+} addition.

2. Experimental procedures

Polycrystalline samples with nominal composition $Na_{0.8}Zn_xCo_{1-x}O_2$ ($0 \leq x \leq 0.15$) were prepared by solid state reaction. A powder mixture of stoichiometric amount of Na_2CO_3, Co_3O_4 and ZnO was directly introduced into a preheated furnace at 850 °C to minimize Na evaporation and held for 16 h in air. The resulting powder was then pulverized, pressed into pellets and sintered at 870 °C for 20 h in air. X-ray powder diffraction with Cu Kα radiation was used to evaluate crystal structure of the sintered parts. The diffraction spectra were fitted employing the "whole powder pattern modelling" (WPPM) approach in which a predefined crystallographic model is not a prerequisite. The thermopower and resistivity of the samples were simultaneously measured using ULVAC-ZEM3 system. In addition, specific heat measurement was carried out employing NETZSCH DSC 404 C system to investigate possible structural transition accompanied with the addition of Zn^{2+} and its influence on the TE properties.

3. Results and discussion

Quantitative determination of the solubility limit x^* of Zn^{2+} in $Na_{0.8}Zn_xCo_{1-x}O_2$ is essential prior to the analysis of its transport properties. X-ray diffraction patterns for polycrystalline $Na_{0.8}Zn_xCo_{1-x}O_2$ ($0 \leq x \leq 0.15$) are shown in Fig. 1(a). The spectra indicate that the $x = 0.00$ and 0.01 samples are a single phase which is indexed with hexagonal cell in the space group $P6_3/mmc$, while samples with $x \geq 0.015$ exhibit additional peaks that are

---

[*] Corresponding author. Tel.: +61 2 9385 5986; fax: +61 2 9385 5956.
E-mail address: sean.li@unsw.edu.au (S. Li).

0925-8388/$ – see front matter © 2011 Elsevier B.V. All rights reserved.
doi:10.1016/j.jallcom.2011.02.045

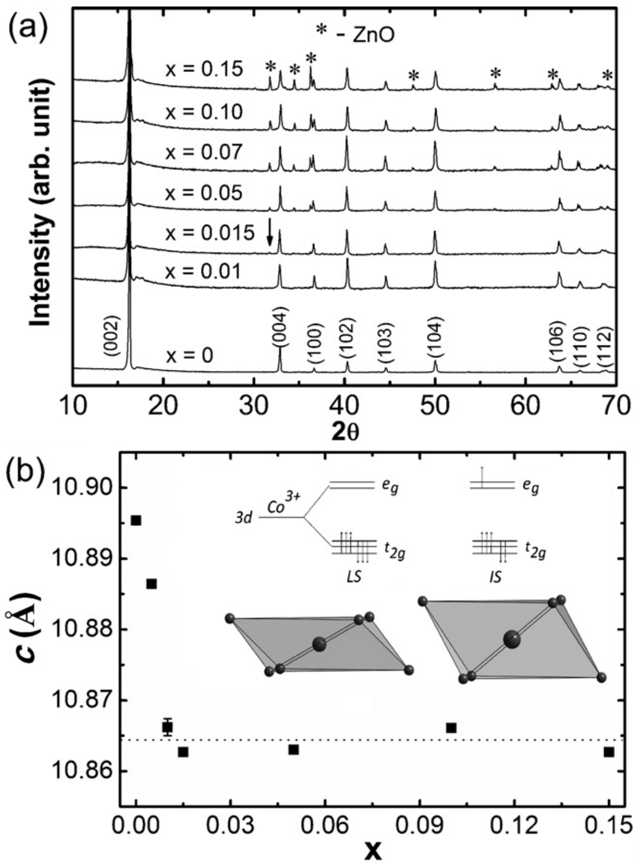

Fig. 1. (a) X-ray powder diffraction spectra for polycrystalline samples with nominal composition $Na_{0.8}Zn_xCo_{1-x}O_2$ and (b) variation of lattice parameter c as a function of x. The inset shows the schematic drawing of one-electron energy level diagram for a low-spin (LS) and an intermediate-spin (IS) Co^{3+} ion as well as the structural modulation of CoO_6 octahedron associated with the ion.

attributed to the presence of secondary ZnO phase, suggesting $0.01 \le x^* < 0.015$. The large discrepancy in x^* between an earlier study [14] and the present study may be due to a difference in atmospheres used (O_2 in Ref. [12] and air in present work) during the fabrication of samples. Our preliminary experiments reveal that both changing the Na content and employing sol–gel technique for sample synthesis appear to be ineffective in raising x^*. Due to the possibility that the low x^* may lie within detection limit of the instrument, crystallographic information was extracted from the diffraction spectra employing the Le Bail refinement (i.e. WPPM approach). Although the increment in lattice parameter a with x is negligible (i.e. within the error limit), the variation of lattice parameter c is rather prominent as illustrated in Fig. 1(b). A significant shrinkage along c-axis direction was observed by 1% Zn-doping, above which the lattice parameter is hardly dependent on x. It is difficult to understand why the shrinkage occurred as Zn^{2+} has a larger radius than the substituted Co^{3+} ions. Similar phenomenon was also observed in Y-substituted ceria electrolyte [20]. For each Co^{3+} substituted by Zn^{2+}, an electronic hole is created (i.e. Co^{4+} ion), which induces localized strain field that breaks the cubic symmetry of its six nearest low-spin LS Co^{3+} ($S = 0$, $t_{2g}^6 e_g^0$) ions, resulting in a reduced energy gap between the highest t_{2g} triplet and lower e_g doublet. This stabilizes intermediate-spin (IS) Co^{3+} ($S = 1$, $t_{2g}^5 e_g^1$) ions [see inset of Fig. 1(b)] [21]. It was considered that an increase in the number of occupation of e_g orbitals with odd number of electrons (i.e. IS Co^{3+} concentration) induced by Zn-doping may favor Jahn–Teller distortion that results in subtle elongation of two of the six Co–O bonds along the c-axis direction. In addition, the larger ionic radius of Zn^{2+} also increases the thickness of CoO_2 layers slightly [see inset of Fig. 1(b)]. The crystal structure of sodium cobaltates consists of edge-sharing CoO_6 octahedra that form CoO_2 layers, between which Na ions are intercalated. An increase in the thickness of CoO_2 layers arising from Jahn–Teller distortion and the substitution of Zn^{2+} for Co^{3+} would consequently lead to a stronger Coulomb attractive force between Na^+ and O^{2-} ions, causing the lattice parameter c to decrease gradually with x, supporting the notion that the Zn^{2+} ions have substituted the Co^{3+} ions in $Na_{0.8}CoO_2$. Although it is also possible that the variation in lattice parameter c may originate from the formation of oxygen vacancies, further investigation reveals that the effect of oxygen vacancies on the lattice parameters is very limited in present case. In this work, x^* is identified to be ~0.01. Thus, raising $x > 0.01$ results in the formation of $Na_{0.8}Zn_{0.01}Co_{0.99}O_2/(ZnO)_y$ composites. Samples are labelled according to the x (Zn-doped) and y (ZnO-added) values. Sample with nominal composition $Na_{0.8}Zn_{0.02}Co_{0.98}O_2$, for instance, will become $Na_{0.8}Zn_{0.01}Co_{0.99}O_2/(ZnO)_{0.01}$.

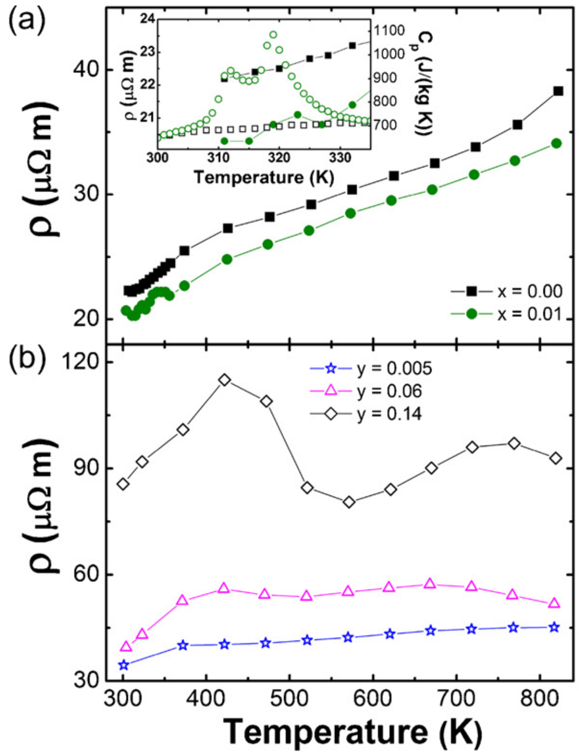

Fig. 2. Temperature dependence of resistivity ρ for (a) Zn-doped $Na_{0.8}Zn_xCo_{1-x}O_2$ and (b) ZnO-added $Na_{0.8}Zn_{0.01}Co_{0.99}O_2/(ZnO)_y$ composites. The inset shows ρ and specific heat (C_p) at near ambient temperature range for the Zn-doped samples. Symbols □ and ○ denote C_p signatures for the $x = 0.00$ and 0.01 samples, respectively.

The resistivity as a function of temperature $\rho(T)$ for Zn-doped $Na_{0.8}Zn_xCo_{1-x}O_2$ and ZnO-added $Na_{0.8}Zn_{0.01}Co_{0.99}O_2/(ZnO)_y$ composites is shown in Fig. 2(a) and (b), respectively. For Zn-doped samples, ρ increases with T. Such metallic behavior is a result of impaired carrier mobility due to enhanced electron-phonon interaction as T is raised. The charge deviation of the system from neutrality caused by the substituted Zn^{2+} is compensated by either increasing: (1) Co^{4+} concentration or (2) oxygen vacancy concentration. The latter, however, is unlikely as oxygen deficiency would reduce the number of carriers as a consequence of electron–hole recombination and impair carrier mobility due to the deterioration of conduction paths within CoO_2 layers, subsequently leading to an increased or a doping-independent ρ. Provided that the charge neutrality of the system is stabilized by the former, the hole concentration n should be raised by 1.25% for the $x = 0.01$

sample in comparison with that for the $x = 0.00$ sample, since $Na_{0.8}Co^{3+}_{0.8}Co^{4+}_{0.2}O_2$ has become $Na_{0.8}Zn_{0.01}Co^{3+}_{0.79}Co^{4+}_{0.2025}O_2$. Yet the result shows a relatively larger reduction in ρ (~10%), suggesting that the reduction in ρ mainly results from enhanced mobility of carriers through Zn^{2+} substitution. Indeed, similar observation was also reported for Cu-substituted $NaCo_{2-x}Cu_xO_4$ where the carrier concentration remains almost unchanged by divalent substitution for Co^{3+} ions [22]. An anomaly in ρ was observed at ~323 K for the $x = 0.01$ sample [(inset of Fig. 2(a)] corresponding to the temperature at which long-range spatial ordering of Na ions takes place. Results from specific heat (C_p) measurement, which are also shown in the inset, register two first-order endothermic peaks for the $x = 0.01$ sample (indicated by ○) attributed to Na ordering and reordering in the temperature range from 310 to 320 K, whereas no such peaks were observable for the undoped sample (indicated by □). The absence of the peaks for the undoped sample may be due to evaporation of Na during sample fabrication, as Na-ordering is normally observed in Na-rich compounds (i.e. ≥0.75) [23]. The C_p of all the composite samples also exhibits identical endothermic peaks at similar temperatures. The Na-ordering temperature is in excellent agreement with that reported in single crystal $Na_{0.75}CoO_2$ [23], which was demonstrated to be due to formation of tri-vacancy superstructure of Na ions. Interestingly, our experimental results suggest that an increase in the concentration of Co^{4+} ions could stabilize Na-ordering. This contradicts with the reported conclusion that Na-ordering is usually observable in Na-rich compounds where the concentration of Co^{4+} ions is small [23]. On the basis of these experimental observations, it was considered that the organizational mechanism for spontaneous Na-ordering is highly two-dimensional (i.e. only within Na layers) and not susceptible to electrostatic potential from neighboring CoO_2 layers.

In contrast to the Zn-doped samples, $\rho(T)$ for ZnO-added $Na_{0.8}Zn_{0.01}Co_{0.99}O_2/(ZnO)_y$ composites exhibits a remarkably different behavior as shown in Fig. 2(b). The secondary ZnO phase mainly resides at grain boundaries of the cobaltates. The interfaces of p-type $Na_{0.8}Zn_{0.01}Co_{0.99}O_2$ and n-type ZnO experience drastic reduction in the number of carriers due to annihilation of electrons and holes, causing ρ to increase with y. In addition, the gradual development of two maxima with increasing y reflects the nature of electron transport in n-type ZnO. It appears that the temperature at which the lower-temperature maximum takes place (T_{m1}) is irrespective of y (~ at 420 K), while the temperature for the higher-temperature maximum (T_{m2}) is dependent on y and reaches 770 K for $y = 0.14$ sample. Lattice dynamical investigation on bulk ZnO reveals that the onset of multi-phonon scattering takes places at 332 and 541 cm^{-1} [24], corresponding to 477 and 778 K respectively. The rough agreement of T_{m1} and T_{m2} with the corresponding temperatures at which the multi-phonon scatterings become active as reported in open literatures may indicate that the maxima seen in Fig. 2(b) could be attributed to the enhanced scattering of electrons with anharmonic lattice vibrations that deteriorate electron mobility, giving rise to an increased ρ at the corresponding temperatures.

The temperature dependences of thermopower $S(T)$ of the Zn-doped and ZnO-added composite samples are plotted in Fig. 3(a). The influence of Na-ordering on S is negligible considering that majority of carriers and their associated hopping is in the electronically conductive CoO_2 layers. S for $Na_{0.8}Zn_{0.01}Co_{0.99}O_2/(ZnO)_y$ composites augments slightly with y. Although S in intrinsic ZnO is negative, the reduction of carrier density related to the electron–hole recombination at the $Na_{0.8}Zn_{0.01}Co_{0.99}O_2$/ZnO interfaces helps to retain the strong Hubbard potential required for the spin and orbital degrees of freedom that enhances S [3]. The most remarkable feature is the simultaneous enhancement of S and the reduction of ρ appeared in the Zn-doped (i.e. $x = 0.01$) sample, which is difficult to interpret within the framework of rigid-band model. In order to shed light on such exotic phenomenon, the transport properties are expressed in terms of Peltier conductivity $\alpha(T) = S(T)/\rho(T)$ for all samples [Fig. 3(b)]. It is discernible that, unlike ρ and S, α is almost temperature independent and that the substitution of Zn^{2+} enhances α while the presence of ZnO seriously deteriorates α over the entire temperature range investigated. Considering the generalized Heikes theory [3], the increase in configurational degeneracy g associated with spin-state transition of Co^{3+} from LS ($g = 1$) to IS ($g = 18$) [25] would induce a backflow of spin entropy that reduces the overall S, providing that the spin state of LS Co^{4+} ($g = 6$) remains intact. Such theoretical prediction has successfully accounted for the negative S value induced by hole carriers in p-type $CaMn_{3-x}Cu_xMn_4O_{12}$ [26]. However, deviation of our experimental observation from the theory suggests that the presence of another dominant mechanism may compensate for the reduction of S resulting from the backflow of spin entropy. The exact mechanism for the overall enhancement of thermopower is not clear at this moment. One possibility is as following. Due to the closed-shell nature of Zn^{2+} ($t^6_{2g}e^4_g$) as well as restriction of the conservation of Hubbard energy, it is unlikely that the substituted Zn^{2+} will contribute to the transport of carriers and its associated entropy. The increased thickness of CoO_2 layers due to Zn^{2+} substitution would relax the c-axis-compressed CoO_6 octahedra with trigonal D_{3d} symmetry towards cubic O_h symmetry, leading to a smaller Co–O–Co bond angle and thus narrower band width. In addition, the ρ measurement [Fig. 2(a)] suggests that the reduction of ρ mainly stems from enhanced carrier mobility while the carrier concentration is much less affected by Zn^{2+} substitution. The nearly doping-independency of carrier concentration is essential for retaining strong Coloumb interaction [3]. The smaller Co–O–Co bond angle, narrower band width and nearly unchanged carrier concentration may lead to a more profound S enhancement [3] that offsets the backflow of entropy resulting from the increased configurational degeneracy of Co^{3+} ions, as observed in Fig. 3(a) and (b).

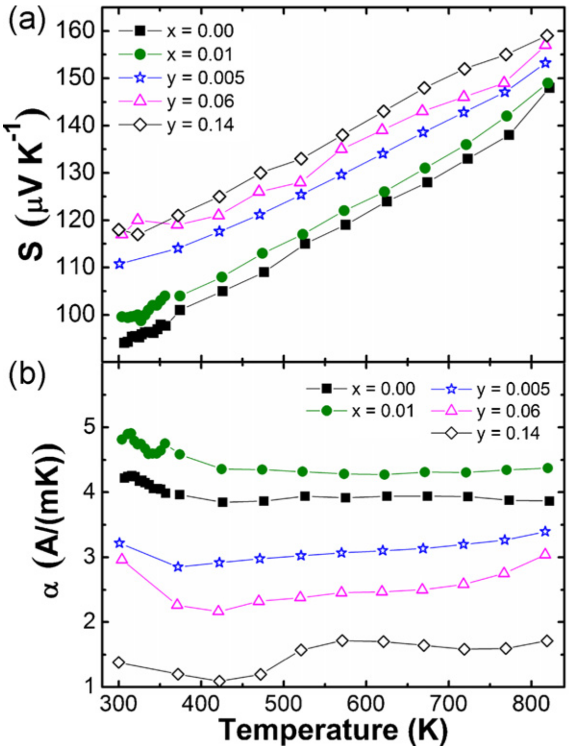

Fig. 3. Temperature dependence of (a) thermopower S and (b) Peltier conductivity α for Zn-doped $Na_{0.8}Zn_xCo_{1-x}O_2$ and ZnO-added $Na_{0.8}Zn_{0.01}Co_{0.99}O_2/(ZnO)_y$ composites.

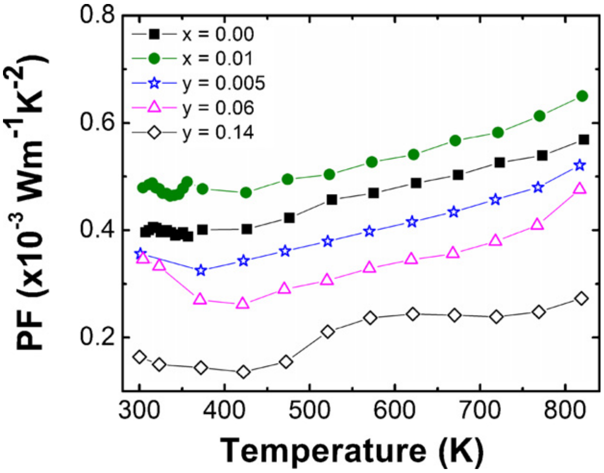

Fig. 4. Thermoelectric power factor (PF) as a function of temperature for Zn-doped $Na_{0.8}Zn_xCo_{1-x}O_2$ and ZnO-added $Na_{0.8}Zn_{0.01}Co_{0.99}O_2/(ZnO)_y$ composites.

The power factor ($PF = S^2/\rho$) for the Zn-doped and ZnO-added composite samples as a function of temperature is illustrated in Fig. 4. It can be seen that PF of all samples increases with T. The highest PF was realized by the sample with $x = 0.01$ and reaches $0.65 \times 10^{-3}\,Wm^{-1}\,K^{-2}$ at ~820 K. A substantial enhancement of PF ~ 20% was achieved by doping Zn^{2+} within x^* (i.e. $x = 0.01$ sample) in comparison with that of its undoped counterpart at 820 K. The presence of ZnO in the host material, however, seriously lowers PF and the effect becomes progressively intense with y. More than two-fold deterioration in PF was realized by the $y = 0.14$ sample.

4. Conclusions

In summary, the thermoelectric properties of $Na_{0.8}Zn_xCo_{1-x}O_2/(ZnO)_y$ ($x \leq 0.01$, $0 \leq y \leq 0.14$) have been systematically investigated. Experimental results suggest that the solubility limit of Zn^{2+} in $Na_{0.8}Zn_xCo_{1-x}O_2$ is 0.01. Doping within the limit leads to simultaneous enhancement of thermopower and reduction of resistivity, resulting in a remarkable enhancement of power factor ~20% in comparison with its undoped counterpart. Possible mechanism for such exotic phenomenon is discussed. Adding x above the limit gives rise to the formation of $Na_{0.8}Zn_{0.01}Co_{0.99}O_2/(ZnO)_y$ composites that drastically deteriorate the thermoelectric performance due to n-type nature of ZnO. The experimental results suggest that extending the solubility limit of Zn in sodium cobaltates presumably employing wet chemical approaches may provide opportunities for further enhancing its thermoelectric properties.

Acknowledgement

This work was financially supported by Australian Research Council Discovery Program (grant no. DP0988687).

References

[1] I. Terasaki, Y. Sasago, K. Uchinokura, Phys. Rev. B 56 (1997) R12685.
[2] K. Takada, H. Sakurai, E. Takayama-Muromachi, F. Izumi, R.A. Dilanian, T. Sasaki, Nature 422 (2003) 53.
[3] W. Koshibae, S. Maekawa, Phys. Rev. Lett. 87 (2001) 236603.
[4] M. Lee, L. Viciu, L. Li, Y. Wang, M.L. Foo, S. Watauchi, R.A. Pascal Jr., R.J. Cava, N.P. Ong, Nat. Mater. 5 (2006) 537.
[5] P.H. Tsai, T. Norby, T.T. Tan, R. Donelson, Z.D. Chen, S. Li, Appl. Phys. Lett. 96 (2010) 141905.
[6] M. Ito, D. Furumoto, J. Alloys Compd. 450 (2008) 494.
[7] M. Ito, D. Furumoto, J. Alloys Compd. 450 (2008) 517.
[8] M. Ito, T. Nagira, S. Hara, J. Alloys Compd. 408 (2006) 1217.
[9] T. Nagira, M. Ito, S. Katsuyama, K. Majima, H. Nagai, J. Alloys Compd. 348 (2003) 263.
[10] K. Park, K.U. Jang, H.C. Kwon, J.G. Kim, W.S. Cho, J. Alloys Compd. 419 (2006) 213.
[11] A.V.S. Tosawat, B. Thanusit, M. Santi, K. Ken, M. Hiroaki, U. Masayoshi, Y. Shinsuke, J. Alloys Compd. 407 (2006) 314.
[12] L. Wang, M. Wang, D. Zhao, J. Alloys Compd. 471 (2009) 519.
[13] K. Park, J.H. Lee, Mater. Lett. 62 (2008) 2366.
[14] P. Mandal, J. Appl. Phys. 104 (2008) 063902.
[15] R. Kitawaki, I. Terasaki, J. Phys.: Condens. Matter 14 (2002) 12495.
[16] S. Li, R. Funahashi, I. Matsubara, S. Sodeoka, Mater. Res. Bull. 35 (2000) 2371.
[17] T. Zhou, D. Zhang, T.W. Button, F.J. Berry, C. Greaves, Dalton Trans. 39 (2010) 1089.
[18] P. Strobel, H. Muguerra, S. Hebert, E. Pachoud, C. Colin, M.-H. Julien, J. Solid State Chem. 182 (2009) 1872.
[19] Z. Zhang, J. Zhang, Y. Xu, C. Jing, S. Cao, Y. Zhao, Phys. Rev. B 74 (2006) 045108.
[20] T.S. Zhang, J. Ma, H.T. Huang, P. Hing, Z.T. Xia, S.H. Chan, J.A. Kilner, Solid State Sci. 5 (2003) 1505.
[21] M. Daghofer, P. Horsch, G. Khaliullin, Phys. Rev. Lett. 96 (2006) 216404.
[22] I. Terasaki, I. Tsukada, Y. Iguchi, Phys. Rev. B 65 (2002) 195106.
[23] M. Roger, D.J.P. Morris, D.A. Tennant, M.J. Gutmann, J.P. Goff, J.U. Hoffmann, R. Feyerherm, E. Dudzik, D. Prabhakaran, A.T. Boothroyd, N. Shannon, B. Lake, P.P. Deen, Nature 445 (2007) 631.
[24] N. Ashkenov, B.N. Mbenkum, C. Bundesmann, V. Riede, M. Lorenz, D. Spemann, E.M. Kaidashev, A. Kasic, M. Schubert, M. Grundmann, G. Wagner, H. Neumann, V. Darakchieva, H. Arwin, B. Monemar, J. Appl. Phys. 93 (2003) 126.
[25] W. Koshibae, K. Tsutsui, S. Maekawa, Phys. Rev. B 62 (2000) 6869.
[26] W. Kobayashi, I. Terasaki, M. Mikami, R. Funahashi, J. Phys. Soc. Jpn. 73 (2004) 523.